Published in final edited form as:
JACC Cardiovasc Imaging. 2012 August ; 5(8): 789–797. doi:10.1016/j.jcmg.2011.12.024.

Magnetic Resonance Cine DENSE Dyssynchrony Parameters for the Evaluation of Heart Failure: Comparison to Myocardial Tissue Tagging

Loren P. Budge, M.D.[1,*], **Adam Helms, M.D.**[1,*], **Michael Salerno, M.D., PhD**[1], **Christopher M. Kramer, M.D., F.A.CC.**[1], **Frederick H. Epstein, Ph.D.**[2], and **Kenneth C. Bilchick, M.D., M.S., F.A.C.C.**[1]

[1]Department of Medicine, University of Virginia Health System, Charlottesville, Virginia

[2]Department of Biomedical Engineering, University of Virginia Health System, Charlottesville, Virginia

Abstract

Objective—We sought to assess the effectiveness of automated mechanical dyssynchrony (MD) parameters based on regional heterogeneity of strain (circumferential (CURE), longitudinal (LURE), and radial (RURE) uniformity ratio estimates) relative to parameters based on regional time to peak contraction using cardiac magnetic resonance (CMR) cine DENSE (Displacement Encoding with Stimulated Echoes) validated with myocardial tissue tagging (MTT) strain data.

Background—Dyssynchrony measures based on the Fourier transformation (FT) of regional strain, such as CURE (previously evaluated in CRT candidates), directly assess MD and yield straightforward global dyssynchrony indices; however, performance relative to the 12-segment standard deviation in time to peak strain (SD12) or maximal regional delay in time to peak strain is unknown.

Methods—Cine DENSE and MTT were obtained using CMR (1.5T Siemens Avanto) in 13 canines: 3 normal controls, 5 with tachycardia pacing-induced heart failure (HF) and left bundle branch ablation (LBBB-HF), and 5 with HF and narrow QRS (NQRS-HF). Strain and dyssynchrony parameters were determined using both CMR methods.

Results—Both HF groups had reduced peak strains and left ventricular ejection fraction (LVEF) compared to normal cases. There was strong agreement between cine DENSE and MTT based on intraclass correlation coefficients (ICC[95%CI]) (CURE:0.99[0.96,1.00]; LURE:0.92[0.77,0.98]; E_{CC}:0.95[0.72,0.99]; E_{LL}:0.82[0.42, 0.97]). FT-based metrics (scale 0–1), in particular CURE, discriminated highly between LBBB-HF and NQRS-HF groups (median difference[95%CI]; CURE:0.60[0.43,0.76]; LURE:0.39[0.19,0.58]; RURE:0.22[0.04,0.40]). In contrast, relative confidence intervals for group differences in time-to-peak parameters were wide, indicating less consistent discrimination (median difference[95%CI]; SD12-E_{CC}:52.5[-4.0,109.2]; SD12-E_{LL}: 40.9[-5.3,87.1]; SD12-E_{RR}:42.0[0.4, 83.6]). Correlations between FT-based and time-to-peak

Address for Correspondence: Kenneth Bilchick, M.D., M.S., UVA Health System, Cardiovascular Division, P.O. Box 800158, Charlottesville, VA 22908, tel 434-924-2465, fax 815-346-5805, bilchick@virginia.edu.
*Authors contributed equally

parameters were significant (CURE/SD12-E_{CC}:r=-0.62, p=0.03; LURE/SD12-E_{LL}:r=-0.76, p=0.005), but not as tight as correlations between time-to-peak parameters.

Conclusions—Automated FT-based circumferential, radial, and longitudinal dyssynchrony measures compare favorably with time-to-peak parameters. Cine DENSE was effective for this application and validated with MTT. Further clinical evaluation in CRT candidates using CMR or other imaging modalities is warranted.

Keywords

Magnetic Resonance Imaging; Cardiac Resynchronization Therapy; Heart Failure

Introduction

The overall benefit of cardiac resynchronization therapy (CRT) to selected patients with heart failure (HF) has been shown in clinical trials (1–4), but the nonresponse rate to CRT using current clinical indications is still significant at approximately 30–40% (5). Although other biological factors are involved in CRT response (6), cardiac imaging remains the best studied tool to achieve more accurate identification of CRT responders. Even so, a number of early mechanical dyssynchrony parameters were unable to identify CRT responders effectively in a multicenter clinical trial (5). Although these results have led some to question whether cardiac imaging can identify patients most likely to respond to CRT, an alternative response has been to look for more effective imaging techniques and approaches for CRT patients. For example, there have been promising results shown for echo speckle tracking (7), 3-D echo (8), and cardiac magnetic resonance (CMR) with myocardial tissue tagging (MTT) (9). MR cine DENSE (Displacement Encoding with Stimulated Echoes) is another imaging approach with high potential. DENSE encodes tissue displacement directly into the phase of the MR signal (10), provides high spatial resolution, accurately assesses circumferential, longitudinal, and radial strain, provides rapid strain analysis (11), and offers automatic contouring (12) without the need for tag detection or a minimum tag density.

In addition to the imaging modality used, the parameterization of dyssynchrony is also an important factor. Widely used dyssynchrony parameters are based on time to peak contraction, indexed as the delay in opposing walls or standard deviation for 12 segments (7, 13–15). Although associated studies have shown positive results, identification in peaks in tissue velocity or strain curves may be time-consuming, subjective, and very difficult (or impossible) for segments with infarction, akinesis, dyskinesis, or very low maximum contractile strain. An alternative approach (not specific to CMR) is the use of automated global circumferential (circumferential uniformity ratio estimate/CURE) (9, 16), radial (radial uniformity ratio estimate/RURE), and longitudinal (longitudinal uniformity ratio estimate/LURE) dyssynchrony indices, which are based on the Fourier transformation (FT) of regional strain (FT-based parameters) and do not require assessment of regional strain or velocity peaks.

In the present study, we aimed to assess the hypotheses that FT-based parameters would perform better than corresponding timing-based parameters and that cine DENSE would be feasible and valid for this application based on comparison with MTT. We elected to compare these indices in a validated animal model of HF with and without left bundle branch block (LBBB) rather than in a human CRT study. Because HF with dyssynchrony modeled this way has been shown to improve with resynchronization (16), it was an ideal model to test our hypotheses. Although the study was implemented using CMR, the findings of this study may be extended to any imaging technique that can generate regional strain curves from standard short-axis and long-axis slices.

Methods

Animal Model

Approval for the study was obtained through the University of Virginia Animal Care and Use Committee. As a validated model of dyssynchronous HF (17), we performed left bundle branch ablation (50W, temperature ≤ 60°) prior to tachycardia pacing (LBBB-HF) using a 4mm-tip ablation catheter in 5 canines, resulting in widening of the QRS duration from 55–60 ms to approximately 120 ms with a typical LBBB appearance. Persistence of LBBB was confirmed after a 30-minute waiting period, as well as at the time of final MR examination. Cardiomyopathy was induced in a total of 10 canines with right atrial tachy-pacing at 180 bpm for 5 weeks [the 5 LBBB-HF animals and 5 animals without left bundle ablation (NQRS-HF)]. Three normal canines did not undergo ablation or tachy-pacing.

CMR Protocol

Using a 1.5T Avanto scanner (Siemens Medical Solutions, Erlangen, Germany) with a 4-channel phased-array chest radiofrequency coil, we performed cine DENSE imaging in standard short-axis and long-axis planes in two orthogonal directions for each plane with the following parameters (10, 18): interleaved spiral readout with 6 interleaves per image; repetition time(TR)/echo time(TE) 17ms/1.9ms; section thickness 8 mm; field of view 350 × 350 mm; flip angle 15°; pixel size 2.8 × 2.8 mm; fat suppression; echo spacing 17 ms with view sharing; and displacement-encoding frequency 0.1 cycles/mm. MTT images were obtained using a gradient echo grid tagging sequence: tag spacing 7 mm; TR/TE 8.7/4.2ms; slice thickness 8 mm; field of view 250 × 250 mm; flip angle 14°; pixel size 1.4 × 1.0 mm; and temporal resolution 17.5 ms with view sharing (19).

Image Analysis and Calculation of Dyssynchrony Metrics

Following image acquisition, segmentation of the left ventricular (LV) myocardium was performed, a phase-unwrapping algorithm was applied to LV myocardium pixels, and displacements were calculated (11). Lagrangian strain was computed from displacements in 24 short-axis segments in multiple slices and then projected in both the radial (E_{RR}) and circumferential (E_{CC}) directions relative to the LV center of mass. Longitudinal strain (E_{LL}) was determined by analysis of strain in standard long-axis planes in basal and mid-cavity segments. Left ventricular volumes and ejection fraction were calculated from cine steady-state free precession images using Argus software. Strains were calculated from cine DENSE images using an algorithm developed in Matlab (MathWorks, Natick, MA) and from MTT images using harmonic phase (HARP) analysis software (Diagnosoft Inc., Cary, NC) (11).

Dyssynchrony was assessed by 2 types of analyses for each strain component: variability in time to peak strain and the FT-based uniformity ratio estimates (CURE, LURE, and RURE). Basic timing delays for each strain component were calculated as the difference in time from QRS onset to peak strain for opposing LV segments with earliest and latest peak strain (E_{CC}-Delay, E_{LL}-Delay, and E_{RR}-Delay). The SD12-E_{CC}, SD12-E_{LL}, and SD12-E_{RR} were constructed based on the standard deviation of time to peak strain in 6 basal and 6 mid-cavity segments (12 total segments) similar to the method of Yu used for regional tissue velocity (14).

CURE, LURE, and RURE were calculated as previously described (16). Briefly, this technique involves a simple and automated analysis based on the FT of the spatial distribution of strain. Because synchronous contraction is represented primarily by zero order FT terms and dyssynchronous contraction by first order FT terms, a ratio measure involving these terms (the square root of the ratio of the zero order term to the sum of zero

and first order terms) can be used to index dyssynchrony on a scale between 0 (dyssynchrony) and 1 (synchrony) (9).

Statistical Analysis

The Wilcoxon rank sum test using exact p-values was used to compare continuous variables, while the Hodges Lehmann estimate and exact 95% confidence interval were used to evaluate the median differences between groups. Boxplots were also constructed for a visual comparison of these differences between groups. For pairwise correlations, the Pearson correlation coefficient (r) and associated significance level are reported. Comparison between cine DENSE and MTT was performed using the intraclass correlation coefficients for absolute agreement between methods. Results are presented graphically using both scatter plots with regression lines and Bland-Altman plots. Statistical analysis was performed using SAS 9.2 (Cary, NC).

Results

Animal Model

Successful left bundle branch ablations were completed in all LBBB-HF animals, with resulting QRS durations of 120 ms and characteristic LBBB morphology on the 12-lead electrocardiogram; QRS durations were 55–60 ms in the NQRS-HF group and control groups. After 5 weeks of tachy-pacing, all LBBB-HF and NQRS-HF group animals displayed left ventricular dysfunction with left ventricular ejection fractions (LVEF) < 0.30. The LBBB-HF group showed a trend for lower LVEF (median 0.15 vs. 0.24, p=0.14) and had increased left ventricular end-diastolic volumes (median 110 cc vs. 77 cc, p=0.008) relative to the NQRS-HF group. Normal animals had a greater LVEF than HF animals (median 0.57 vs. 0.15, p=0.017). Examples of CMR steady-state free precession and Lagrangian displacement movies for both a LBBB-HF case and NQRS-HF case may be found in the supplementary video material.

Comparison of cine DENSE and MTT

As shown in Figure 1, agreement between cine DENSE and MTT was excellent for peak E_{CC} (R^2=0.94, p < 0.01; intraclass correlation coefficient for absolute agreement between methods (ICC): 0.95 [95% CI: 0.72,0.99]) and CURE (R^2 = 0.98, p < 0.001; ICC: 0.99 [0.96,1.00]). There was also good agreement between DENSE and MTT for peak E_{LL} (peak E_{LL}: R^2=0.86, p <0.01; ICC: 0.82 [0.42,0.97]) and LURE (R^2 = 0.85, p < 0.001; ICC: 0.92 [0.77,0.98]) (see supplementary material). As previously reported, MTT-based radial strain and dyssynchrony measures were of insufficient precision to include in our analysis (20).

Comparison Between NQRS-HF and LBBB-HF Groups

NQRS-HF and LBBB-HF animals had marked heterogeneity in regional strain curves (see supplementary material for examples of circumferential, longitudinal, and radial regional strain curves for each group). While the regional strain polarity (positive or negative) was generally the same regardless of the strain component for NQRS-HF animals, typical regional strain versus time curves for the LBBB-HF group show simultaneous positive and negative strains in different sectors. This indicates early anteroseptal contraction and lateral wall stretch followed by late lateral wall contraction and anteroseptal stretch. Statistically significant differences in all FT-based parameters (p < 0.01 for CURE and LURE; p=0.016 for RURE) are evident from Table 1, although the magnitude of the difference between LBBB-HF and NQRS-HF groups was greatest for CURE, followed by LURE and RURE (CURE:0.60[0.43,0.76]; LURE:0.39[0.19,0.58]; RURE:0.22[0.04,0.40]).

Boxplots comparing FT-based metrics to corresponding timing-based dyssynchrony parameters (SD12 and opposing wall delay) are shown in Figures 2, 3, and 4 for circumferential, longitudinal, and radial parameters, respectively. From these boxplots, it is evident that while time-to-peak parameters indicate more dyssynchrony for LBBB-HF relative to NQRS-HF cases, the time-to-peak parameters are less consistent within each group (relative to FT-based parameters). The less consistent discrimination with time-to-peak parameters is also apparent from Table 1, which shows that even time-to-peak parameters based on 12 segments have much wider confidence intervals (relative to the scale of the parameter) for the median differences between the LBBB-HF and NQRS-HF groups (SD12-E_{CC}:52.5[−4.0,109.2]; SD12-E_{LL}:40.9[−.5.3,87.1]; SD12-E_{RR}:42.0[0.4, 83.6]).

The two LBBB-HF cases in Figure 5 both have significant dyssynchrony and illustrate some of the advantages of FT-based parameters. In panel A, the circumferential and radial strain curves show absent early septal contraction (sometimes seen when left ventricular systolic dysfunction is more severe or infarction is present). CURE and RURE still both correctly indicate significant dyssynchrony, but time-to-peak measures do not because there are no early contractile strain peaks. There is better agreement in dyssynchrony assessments in Panel B, which shows the classic pattern of early septal contraction and early free wall stretch followed by late free wall contraction and late septal stretch.

Comparison Between Normal and Heart Failure Groups

Figures 2, 3, and 4 also show comparisons for all 9 dyssynchrony parameters between normal cases and those with HF. Dyssynchrony parameters in the normal control and NQRS-HF groups are similar, while the LBBB-HF group demonstrates the greatest amount of dyssynchrony. Median differences and confidence intervals for dyssynchrony parameter differences between the LBBB-HF and normal groups are shown in Table 1.

Correlations among Dyssynchrony Metrics

Only moderate (statistically significant) correlations were present between the FT-based and time-to-peak parameters using E_{CC} and E_{LL} (CURE/SD12-E_{CC}: r=−0.62, p=0.03; LURE/SD12-E_{LL}: r=−0.76, p=0.005). As expected, the correlations were tighter between time-to-peak measures (SD12-E_{CC}/E_{CC}-Delay: r=0.95, p<0.001; SD12-E_{LL}/E_{LL}-Delay: r=0.91, p<0.001; SD12-E_{RR}/E_{RR}-Delay: r=0.89, p<0.001;). A table with all the correlation data may be found in the supplementary material.

Discussion

Major Findings

The key findings of this study are: 1) cine DENSE provides high quality dyssynchrony assessments based on circumferential, longitudinal, or radial strain, with good correlation with MTT; 2) cine DENSE assessment of mechanical dyssynchrony in HF using FT-based parameters quantifying the extent of simultaneous myocardial stretch and contraction is feasible; 3) FT-based dyssynchrony parameters (CURE, RURE, and LURE) derived from CMR effectively discriminate HF with and without LBBB and perform favorably relative to time-to-peak parameters.

Timing-based vs. FT-based Dyssynchrony Parameters

Widely used dyssynchrony measures from the echocardiography (7, 13, 14) and CMR literature (15) are dependent on the time to peak contraction. Despite this, with both echocardiography and CMR, determination of time to peak contraction based on regional tissue velocity or strain curves may be difficult when infarction, akinesis, or dyskinesis is present, or when segmental velocity/strain curves have a predominant stretch pattern, low

maximal amplitude and/or multiple peaks. In contrast, FT-based measures such as CURE, LURE and RURE measure the degree to which some segments contract while other segments stretch during the cardiac cycle and do not require manual identification of strain/velocity peaks, providing an automated and easily interpretable global measure of dyssynchrony. Because these FT-based dyssynchrony parameters may be easily determined with any imaging modality that generates strain curves from standard LV short-axis and long-axis views, this methodology has broad potential clinical applicability.

Clinical Importance of Dyssynchrony Assessment by Echocardiography

Early single-center echocardiographic studies using tissue Doppler imaging showed that a significant delay between time to peak systolic velocity at basal septal and basal lateral segments predicted a lower adverse clinical event rate after CRT (13). In addition, an alternative parameterization based on the standard deviation of time from QRS onset to peak systolic velocity for 12 left ventricular segments (derived from tissue Doppler imaging) was also shown to be effective and associated with LV reverse remodeling after CRT (14). Subsequently, the multicenter PROSPECT study “observed relatively low yield and high variability for TDI [tissue Doppler imaging] measures” (5). Although the methodology was criticized by some, the study seemed to have the positive effect of encouraging the development of more advanced echocardiographic dyssynchrony methods with assessments of radial and circumferential strain, such as echo speckle tracking and 3-D echocardiography, and positive clinical studies were subsequently published based on these methods (7, 8). In addition, advanced strain analysis methods based on myocardial tagging (9) and cine DENSE (11, 12) have also been developed for this purpose.

Clinical Impact of Refined Dyssynchrony Imaging

Despite a large number of CRT-related imaging studies, major guidelines for CRT patient selection in patients with a widened QRS do not include any criteria based on imaging (with the exception of the UK National Institute for Health and Clinical Excellence guidelines) (21). In spite of this, significant heterogeneity in CRT response still exists even in patients with a wide QRS, and there are compelling reasons to improve CRT selection criteria in these patients. These include an increased complication rate associated with CRT-D relative to the rate with standard ICDs. For example, in the RAFT study, the complication rate for CRT-D was 13%, which was significantly greater than the complication rate for standard ICDs (22). Procedure times and patient radiation exposure are also increased with CRT (23). In addition, CRT carries considerable costs related to the device, implantation, monitoring, and the need for multiple device changes over a lifetime. Based on these costs and current CRT nonresponse rates, if the medical community does not develop more effective ways to identify the best CRT candidates, it is possible that reimbursement could be restricted in the future, which could leave a number of potential CRT responders unable to receive this treatment.

In light of recent results for speckle tracking, 3-D echocardiography, and CMR modalities such as DENSE and myocardial tagging, it is our opinion that cardiac imaging for mechanical dyssynchrony and viability holds the best promise for developing more meaningful CRT patient selection criteria, although a positive large multicenter randomized trial would be needed to influence guidelines. We believe that effective imaging for mechanical dyssynchrony requires both accurate assessment of cardiac mechanical function and optimal parameterization of the degree of dyssynchrony. Because the present study has addressed both these issues and demonstrated an advantage for FT-based parameters over time-to-peak parameters, we believe this work will have significant clinical impact. Of note, these FT-based dyssynchrony parameters could have potential broad application to strain

data obtained not only from cine DENSE MR but also other imaging modalities capable of generating regional strain curves.

Limitations and Rationale for Translational Approach

This is a translational rather than a clinical study, and our model of LBBB may not be representative of all types of mechanical dyssynchrony in human HF; however, this design provided a controlled and validated model to test our hypotheses. Further clinical investigation is indicated based on these data. Of note, we chose a translational approach for several reasons. First, the model was necessary to demonstrate consistency of cine DENSE and MTT for dyssynchrony and strain assessment. Second, the pacing-induced HF model is a well-validated animal model of HF and produces LV dysfunction similar to the LV dysfunction present in patients referred for CRT (1, 2). Third, induction of LBBB results in the prototypical model of mechanical dyssynchrony (17) that responds to resynchronization based on prior published data (16). Fourth, the translational model has allowed us to determine that this technique has the potential to perform better than timing-based methods in human HF patients, which justifies further clinical study.

Conclusions

Automated FT-based circumferential, radial, and longitudinal dyssynchrony indices based on heterogeneity of regional segmental strain may be easily determined without the need for time-to-peak contraction determinations and compare favorably with time-to-peak parameters. In the present study, we demonstrate the effectiveness of cine DENSE for this purpose, with validation based on strain obtained from HARP analysis of MTT. Further clinical evaluation is warranted using cine DENSE CMR or other imaging modalities, as this methodology may be extended to any imaging modality capable of generating regional strain curves from standard LV short-axis and long-axis views.

Supplementary Material

Refer to Web version on PubMed Central for supplementary material.

Acknowledgments

This work was supported by NIH grants K23 HL094761 (KCB) and R01 EB001763 (FHE)

Drs. Kramer, Epstein, and Salerno have grant support from Siemens. Dr. Kramer is a consultant for St. Jude Medical. Pacemakers designated for animal use were donated by St. Jude Medical.

The authors thank Xiaodong Zhong, PhD., Robert Janiczek, Ph.D., Andrew Gilliam, Ph.D., John Christopher, R.T., and Craig Goodman, B.S., for their assistance.

Abbreviations

CMR	Cardiac Magnetic Resonance Imaging
CRT(-D)	Cardiac Resynchronization Therapy (Defibrillator)
CURE/LURE/RURE	Circumferential/Longitudinal/Radial Uniformity Ratio Estimates
$E_{CC}/E_{LL}/E_{RR}$	Circumferential/Longitudinal/Radial Strain
FT	Fourier Transformation
HF	Heart Failure
LBBB	Left Bundle Branch Block

LVEF	Left Ventricular Ejection Fraction
MTT/HARP Analysis	Myocardial Tissue Tagging/Harmonic Phase Analysis
SD12	Standard deviation of time to peak strain in 12 segments

Reference List

1. Bristow MR, Saxon LA, Boehmer J, et al. Cardiac-resynchronization therapy with or without an implantable defibrillator in advanced chronic heart failure. N Engl J Med. 2004; 350:2140–50. [PubMed: 15152059]
2. Abraham WT, Fisher WG, Smith AL, et al. Cardiac resynchronization in chronic heart failure. N Engl J Med. 2002; 346:1845–53. [PubMed: 12063368]
3. Cleland JG, Daubert JC, Erdmann E, et al. The effect of cardiac resynchronization on morbidity and mortality in heart failure. N Engl J Med. 2005; 352:1539–49. [PubMed: 15753115]
4. Moss AJ, Hall WJ, Cannom DS, et al. Cardiac-resynchronization therapy for the prevention of heart-failure events. N Engl J Med. 2009; 361:1329–38. [PubMed: 19723701]
5. Chung ES, Leon AR, Tavazzi L, et al. Results of the Predictors of Response to CRT (PROSPECT) trial. Circulation. 2008; 117:2608–16. [PubMed: 18458170]
6. Aiba T, Hesketh GG, Barth AS, et al. Electrophysiological consequences of dyssynchronous heart failure and its restoration by resynchronization therapy. Circulation. 2009; 119:1220–30. [PubMed: 19237662]
7. Tanaka H, Nesser HJ, Buck T, et al. Dyssynchrony by speckle-tracking echocardiography and response to cardiac resynchronization therapy: results of the Speckle Tracking and Resynchronization (STAR) study. Eur Heart J. 2010; 31:1690–700. [PubMed: 20530502]
8. Marsan NA, Bleeker GB, Ypenburg C, et al. Real-time three-dimensional echocardiography permits quantification of left ventricular mechanical dyssynchrony and predicts acute response to cardiac resynchronization therapy. J Cardiovasc Electrophysiol. 2008; 19:392–9. [PubMed: 18179529]
9. Bilchick KC, Dimaano V, Wu KC, et al. Cardiac magnetic resonance assessment of dyssynchrony and myocardial scar predicts function class improvement following cardiac resynchronization therapy. JACC Cardiovasc Imaging. 2008; 1:561–8. [PubMed: 19356481]
10. Kim D, Gilson WD, Kramer CM, Epstein FH. Myocardial tissue tracking with two-dimensional cine displacement-encoded MR imaging: development and initial evaluation. Radiology. 2004; 230:862–71. [PubMed: 14739307]
11. Spottiswoode BS, Zhong X, Hess AT, et al. Tracking myocardial motion from cine DENSE images using spatiotemporal phase unwrapping and temporal fitting. IEEE Trans Med Imaging. 2007; 26:15–30. [PubMed: 17243581]
12. Spottiswoode BS, Zhong X, Lorenz CH, Mayosi BM, Meintjes EM, Epstein FH. Motion-guided segmentation for cine DENSE MRI. Med Image Anal. 2009; 13:105–15. [PubMed: 18706851]
13. Bax JJ, Bleeker GB, Marwick TH, et al. Left ventricular dyssynchrony predicts response and prognosis after cardiac resynchronization therapy. J Am Coll Cardiol. 2004; 44:1834–40. [PubMed: 15519016]
14. Yu CM, Fung JW, Zhang Q, et al. Tissue Doppler imaging is superior to strain rate imaging and postsystolic shortening on the prediction of reverse remodeling in both ischemic and nonischemic heart failure after cardiac resynchronization therapy. Circulation. 2004; 110:66–73. [PubMed: 15197148]
15. Westenberg JJ, Lamb HJ, van der Geest RJ, et al. Assessment of left ventricular dyssynchrony in patients with conduction delay and idiopathic dilated cardiomyopathy: head-to-head comparison between tissue doppler imaging and velocity-encoded magnetic resonance imaging. J Am Coll Cardiol. 2006; 47:2042–8. [PubMed: 16697323]
16. Leclercq C, Faris O, Tunin R, et al. Systolic improvement and mechanical resynchronization does not require electrical synchrony in the dilated failing heart with left bundle-branch block. Circulation. 2002; 106:1760–3. [PubMed: 12356626]

17. Bilchick KC, Helm RH, Kass DA. Physiology of biventricular pacing. Curr Cardiol Rep. 2007; 9:358–65. [PubMed: 17877930]

18. Zhong X, Spottiswoode BS, Meyer CH, Kramer CM, Epstein FH. Imaging three-dimensional myocardial mechanics using navigator-gated volumetric spiral cine DENSE MRI. Magn Reson Med. 2010; 64:1089–97. [PubMed: 20574967]

19. Zerhouni EA, Parish DM, Rogers WJ, Yang A, Shapiro EP. Tagging with MR Imaging - A Method for Noninvasive Assessment of Myocardial Motion. Radiology. 1988; 169:59–63. [PubMed: 3420283]

20. Moore CC, Lugo-Olivieri CH, McVeigh ER, Zerhouni EA. Three-dimensional systolic strain patterns in the normal human left ventricle: characterization with tagged MR imaging. Radiology. 2000; 214:453–66. [PubMed: 10671594]

21. UK National Institute for Health and Clinical Excellence. [Accessed November 1, 2011] TA120 Heart failure - cardiac resynchronisation: guidance. Jul. 2010 Available at: http://guidance.nice.org.uk/TA120/Guidance/pdf/English

22. Tang AS, Wells GA, Talajic M, et al. Cardiac-resynchronization therapy for mild-to-moderate heart failure. N Engl J Med. 2010; 363:2385–95. [PubMed: 21073365]

23. Perisinakis K, Theocharopoulos N, Damilakis J, Manios E, Vardas P, Gourtsoyiannis N. Fluoroscopically guided implantation of modern cardiac resynchronization devices: radiation burden to the patient and associated risks. J Am Coll Cardiol. 2005; 46:2335–9. [PubMed: 16360068]

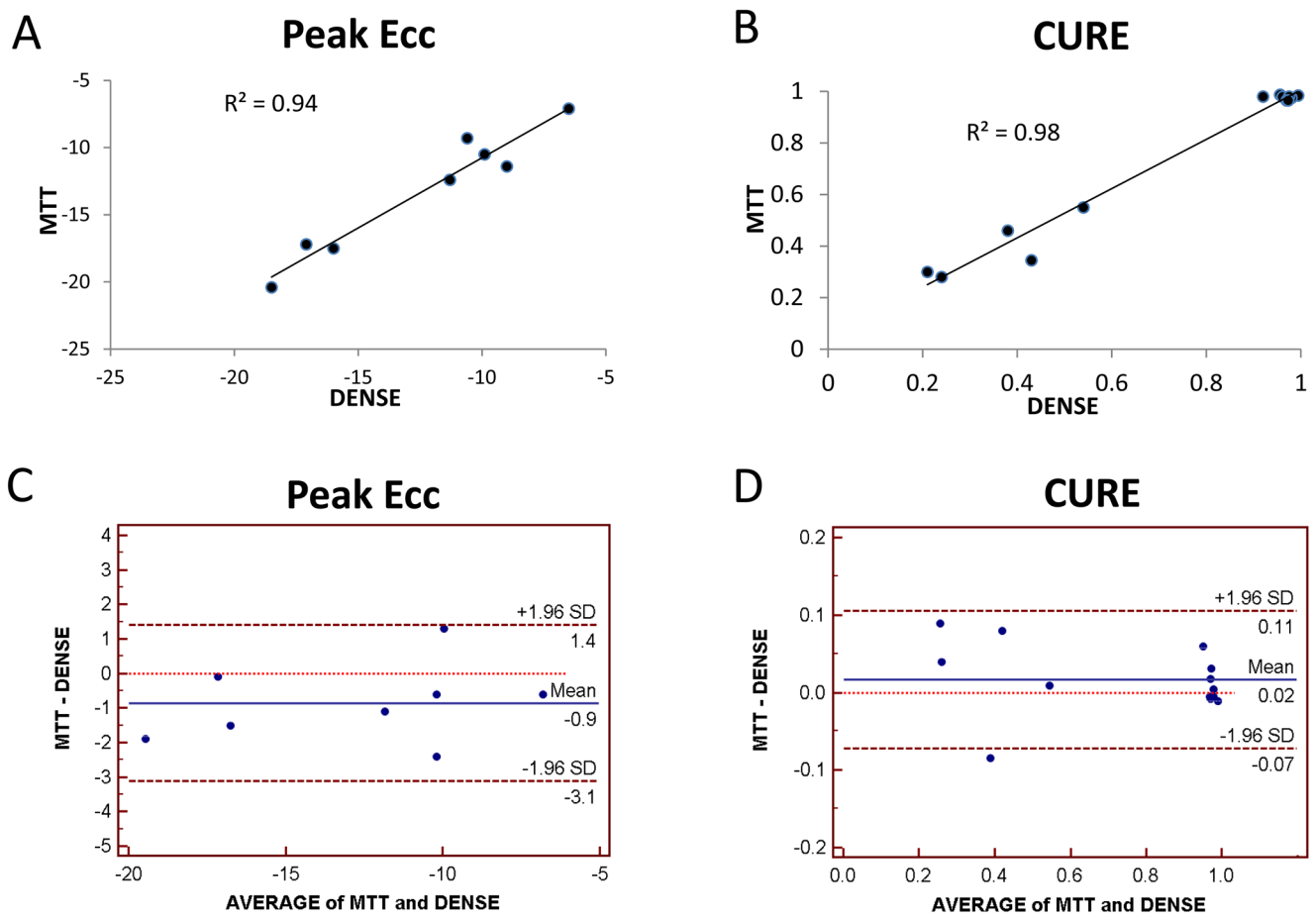

Figure 1. Peak Circumferential Strains and Circumferential Dyssynchrony from Cine DENSE versus Myocardial Tissue Tagging

Correlation between cine DENSE and myocardial tissue tagging is shown for (A) circumferential strain (E_{CC}) and (B) the circumferential dyssynchrony measure CURE. Agreement between the methods is also shown in the form of Bland Altman plots for (C) E_{CC} and (D) CURE.

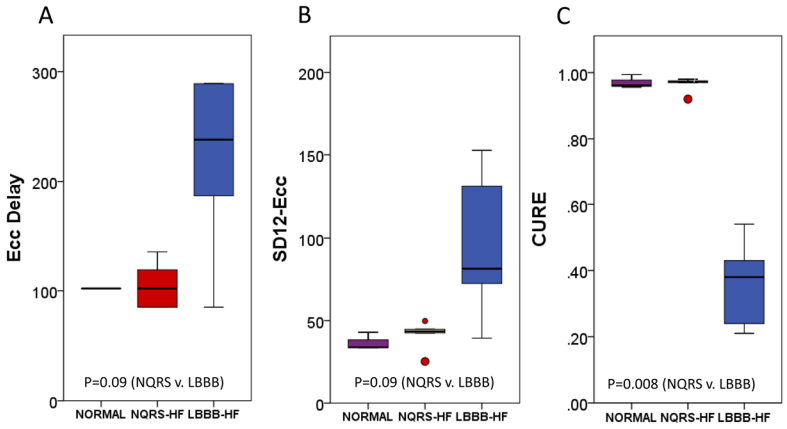

Figure 2. Boxplots of Circumferential Dyssynchrony Parameters

A boxplot comparison of (**A**) E_{CC}-Delay, (**B**) SD12- E_{CC}, and (**C**) CURE in normal, NQRS-HF, and LBBB-HF groups is shown.

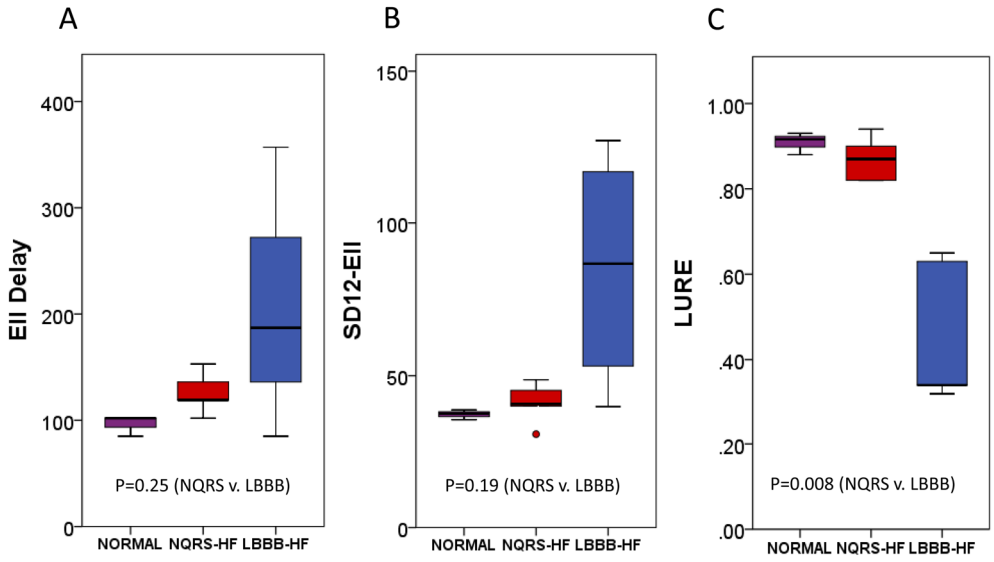

Figure 3. Boxplots of Longitudinal Dyssynchrony Parameters

A boxplot comparison of (**A**) E_{LL}-Delay, (**B**) SD12- E_{LL}, and (**C**) LURE in normal, NQRS-HF, and LBBB-HF groups is shown.

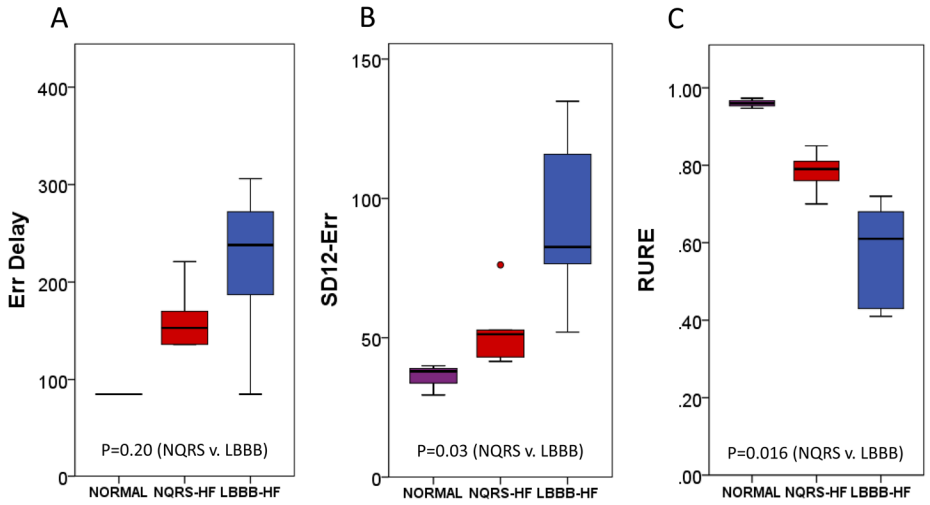

Figure 4. Boxplots of Radial Dyssynchrony Parameters

A boxplot comparison of (**A**) E_{RR}-Delay, (**B**) SD12- E_{RR}, and (**C**) RURE in normal, NQRS-HF, and LBBB-HF groups is shown.

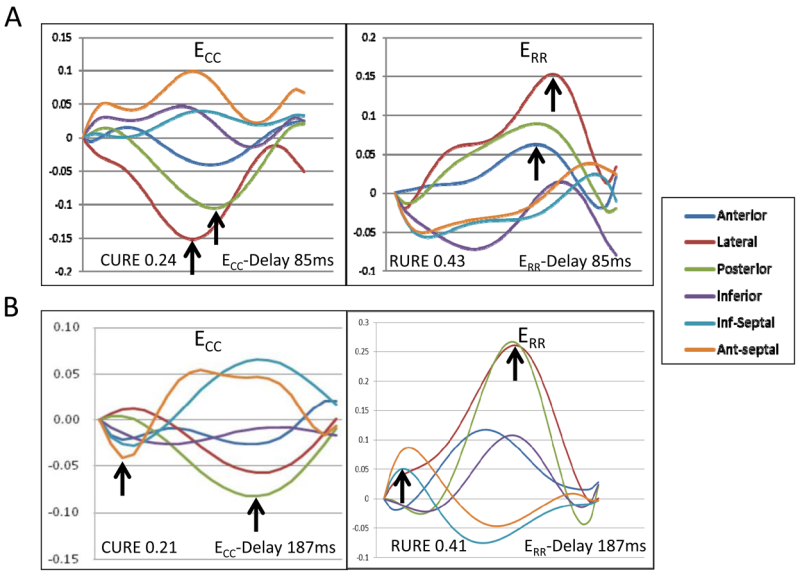

Figure 5. Comparison of LBBB-HF Dyssynchrony Assessments

Both cases have significant dyssynchrony due to HF and LBBB. In the first case (**A**), FT-based measures indicate marked dyssynchrony, but time-to-peak measures do not due to the absence of early contractile strain peaks. In the second case (**B**), both FT-based and time-to-peak parameters indicate a high level of dyssynchrony. In both cases, both types of time-to-peak parameters (delay and SD12 indices) resulted in similar assessments.

Table 1

Differences Among Groups for CMR Dyssynchrony Parameters

	Median Difference for LBBB-HF v. NQRS-HF (Midpoint [95% CI])	p-value	Median Difference for LBBB-HF v. Normal (Midpoint [95% CI])	p-value
CURE (0–1)	0.60 [0.43,0.76]	0.008	0.60 [0.42,0.78]	0.04
LURE (0–1)	0.39 [0.19,0.58]	0.008	0.42 [0.23,0.61]	0.04
RURE (0–1)	0.22 [0.04,0.40]	0.016	0.40 [0.23, 0.56]	0.04
SD12- E_{CC}(ms)	52.5 [−4.0,109.2]	0.09	57.8 [−3.5,119,1]	0.07
SD12- E_{LL}(ms)	40.9 [−5.3,87.1]	0.19	46.4 [1.1,91.6]	0.05
SD12- E_{RR}(ms)	42.0 [0.4,83.6]	0.03	58.8 [12.1,105.5]	0.04
E_{CC}-Delay(ms)	93.5 [−17,204]	0.09	85 [−17,187]	0.25
E_{LL}-Delay(ms)	93.5[−51,238]	0.25	127 [−17,272]	0.31
E_{RR}-Delay(ms)	42.5 [−51,136]	0.20	110.5 [0,221]	0.11